

INVERSE MODELING IN GEOPHYSICAL APPLICATIONS

G. CURRENTI*, R. NAPOLI, D. CARBONE, C. DEL NEGRO, G. GANCI

*Istituto Nazionale di Geofisica e Vulcanologia, Sezione di Catania,
Catania, Italy*

**E-mail: currenti@ct.ingv.it
maglab.ct.ingv.it*

The interpretation of the potential field data is an useful tool that allows for both investigating the subsurface structures and providing a quantitative evaluation of the geophysical process preceding and accompanying period of volcanic unrest. Potential field inversion problem are required to combine forward models with appropriate optimization algorithms and automatically find the best set of parameters that well matches the available observations. Indeed, investigations on the mathematical equations to be inverted, have revealed that these models are ill-posed and highly non-linear. Numerical methods for modeling potential field observations are proposed and applied on real dataset.

Keywords: Geophysical inversion; Potential Field; Mount Etna.

1. Introduction

The inversion problem in potential field modeling suffers from the ambiguity and instability of its solutions. The ambiguity arises from the inherent property of potential fields for which different combinations of parameters may lead to similar anomalies. Moreover, potential fields inversion is notoriously unstable. Because of ambiguity and instability of solutions, the inversion problem can be secured by narrowing the set of all possible solutions to a predefined solution class that allow for a unique and stable solution. The priori definition of the geometry (simplified bodies: spherical, rectangular, prismatic) of searched source and the priori recognition of the involved physical mechanism allows reducing the number of likely solutions considerably.¹ Potential field inversion method can be classified into two main categories depending on the type of the unknown parameters to be retrieved. Firstly, there are some methods looking for magnetization or density contrast values with fixed geometry sources. In this case linear inversion technique can be successfully applied. Secondly, there are those

methods that look for geometrical determinations of the source. In this latter case the inversion problem is highly non-linear and robust nonlinear inversion techniques are needed. The first category of interpretation models is widely used in providing physical property distributions of subsurface geological structures, while the second one is generally applied in modeling potential field sources in volcanic areas. In the following two inversion approaches are described to deal with linear and non-linear inversion problems and are applied on two case studies to appraise the goodness of the proposed methods.

2. 3D linear inversion of potential field data

Potential field inversion are aimed to provide a model which reconstructs, as well as possible, subsurface geological structures having a density/magnetization contrast with their surroundings. For the sake of simplicity, we consider the magnetic inverse problem. However, similar formulation can be applied to the case of gravity inversion method. The computational domain V which is supposed to surround the magnetic source is discretized using a finite number of $m = N_x * N_y * N_z$ rectangular prisms whose magnetization J_j is uniform inside each prism.¹ Using a 3D discrete numerical approach, the total anomaly field at i -th observation point is computed by:

$$T_i = \sum_{j=1}^n J_j a_{ij} \quad (1)$$

where elements a_{ij} quantify the contribution to the total magnetic field anomaly T at i -th observation point due to the magnetization of the j -th prism.² Therefore, the inverse problem can be formulated as the solution of a system of n linear equations as:

$$Ax = T \quad (2)$$

where x is the m vector of unknown magnetization values of the prisms, T is the n vector of observed magnetic data, and A is a matrix with elements a_{ij} . The analytical expression of the a_{ij} term for a prismatic body was devised by Rao and Babu.³ Based on discretization, the number of prisms is usually larger than the number of observation points, thus the linear inverse problem in Eq. (2) turns out to be unavoidably underdetermined. In such a case, the linear system leads to a solution with $m - n$ degree of

freedom. A further difficulty in solving the system in Eq. (2) is due to the inherent non-uniqueness of the potential field: there are an infinite number of inverse models that can explain the same observed magnetic anomaly within error limits. This highlights that the magnetic inverse problem is ill-posed. That calls for some regularization techniques. In such a case, it is necessary to impose further constraints taking into account a priori knowledge about the solution when available. The idea of reducing the class of possible solution to some set on which the solution is stable lies on the fundamental concept of introducing a regularizing operator. The inverse problem can be re-formulated as an optimization problem aimed at finding the unknown magnetization values x that minimize a functional ϕ composed of a data misfit ϕ_d and a smoothing functional ϕ_m :

$$\phi = \phi_d + \phi_m = \frac{1}{2}[(Ax - T_{obs}^T)(Ax - T_{obs}) + \lambda(x - x_0)^T W^T W(x - x_0)] \quad (3)$$

where W is a weighting matrix and λ is the regularization parameter. Because of the lack of depth resolution, W is aimed to counterbalance the contribution of deeper prisms with respect to shallower ones. To ensure that the solution is geologically reasonable it is advisable to prescribe realistic bounds on the magnetization values on the basis of rock samples or available information about the local geology. The minimization of the quadratic functional in Eq. (3) subjected to bound constraints can be solved by using a Quadratic Programming (QP) algorithm based on active set strategy:⁴

$$\min \phi = \min[\frac{1}{2}x^T Qx - d^T x], L \leq x \leq U \quad (4)$$

where $Q = A^T A + \lambda W^T W$ and $d = A^T T + \lambda W^T W x_0$, and L and U are the vectors of lower and upper bounds. The quadratic formulation of the problem is solved iteratively by generating a sequence of feasible solutions that converge toward the optimal solution. The iteration is stopped when no relative improvements in the functional are achieved.

The inversion procedure described above was applied to analyze the anomalies detected by a ground magnetic survey of the Ustica island covering an area of about 9 km². The total-intensity anomaly field, obtained after data reduction process, shows the presence of a W-E striking magnetic anomaly in the middle of the island and other two intense anomalies, which seem to continue offshore, in the south-western and the north-eastern sides (Fig. 1).

4

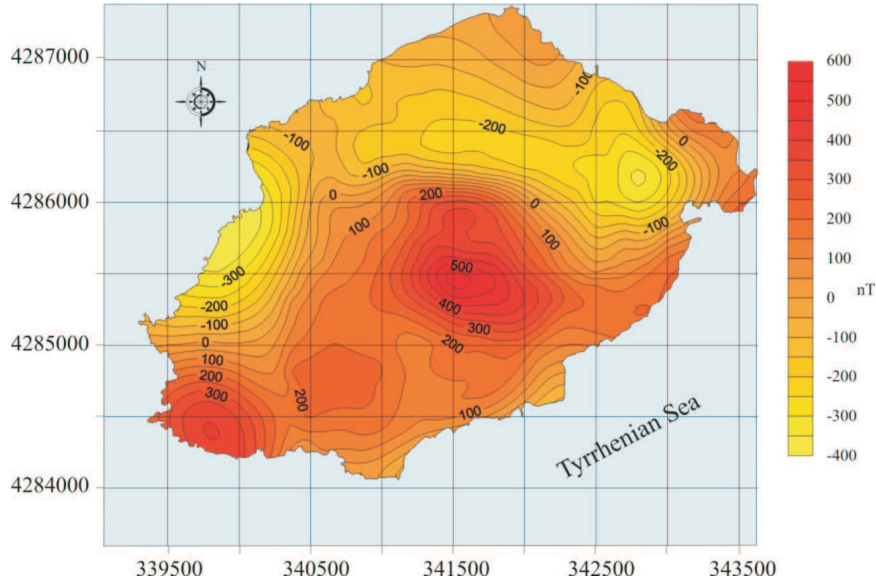


Fig. 1. Map of the total intensity magnetic field after reduction process.

In order to allow the maximum flexibility for the model to represent geologically realistic structures the island was represented as a crustal block, $4 \times 3 \text{ km}^2$ in area and about 1.2 km in thickness, and was discretized into a set of rectangular prisms ($0.125 \times 0.125 \times 0.15 \text{ km}^3$ in size). The anomaly field was inverted assuming that the average direction of total magnetization is close to Earth's present-day field direction (approximate inclination of 54° N , declination of 1° W). Moreover taking advantage of magnetizations measured on volcanic rocks of the island, the inversion of the data set was performed constraining the range of the magnetization value for the assumed sources from 0 to 10 A/m. The iterations were continued until the functional does not show significant improvements. The residual field, the difference between observed field and calculated field is shown in Fig. 2. Only in the N-E and S-W area of the island two small residual anomalies remain probably due to a low resolution of the volume discretization in these zones.

The 3D model resulting from the constrained inversion of data set reveals the presence of three main magnetic trends, N-S, E-W and NE-SW, which are in good agreement with the surface geology, and are coincident with the main regional structural lineaments (Fig. 3).

In particular, the N-S and E-W trends, which are of more recent origin,

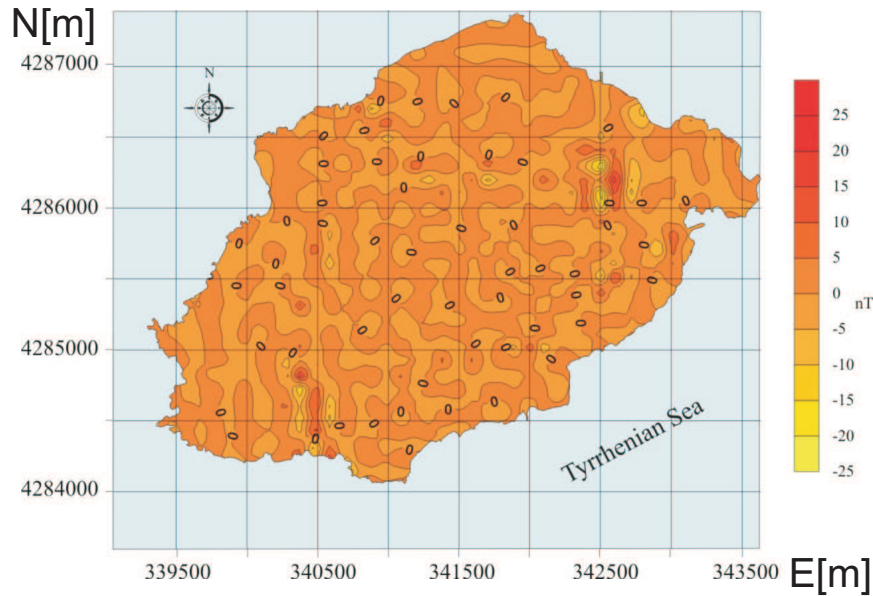


Fig. 2. Residual, total-field magnetic anomaly map produced by subtracting the computed field from observed field.

prevail in the shallow part of the model, while the NE-SW is relevant below 0.4 km b.s.l. At this depth the model reveals a magnetized body in the central area, which may be interpreted as the preferential area for magma storage and ascent and which supplied the feeding systems of the main sub-aerial volcanic centres of the island, Mt. Guardia dei Turchi and Mt. Costa del Fallo. Two other magnetized volumes were identified and ascribed to the small submarine/subaerial eruptive centres of the western island and to the younger cone of Capo Falconiera, respectively. These findings highlight how the regional tectonics has strongly influenced the structural and magmatic evolution of the Ustica volcanic complex producing preferential ways for magma ascents. Moreover, considering that the NE-SW trend prevails only in the deeper part of the model and is replaced at the shallow depths by the N-S and E-W orientations, it is possible to assume that a change of tectonic style and/or its orientation took place in the past⁵.

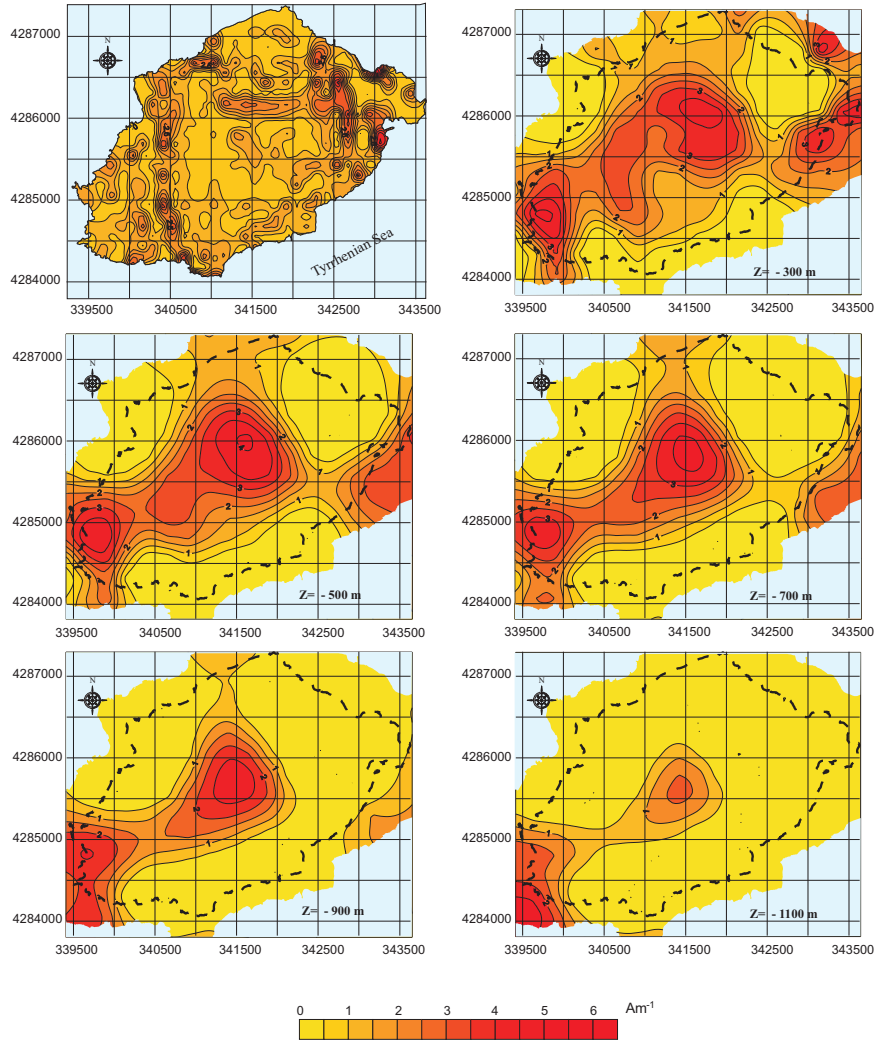


Fig. 3. The 3 D magnetization model of the Ustica volcanic complex. Horizontal sections of the uppermost part (above sea level) of the model and from 300m depth until 1100m depth.

3. Non-linear inversion of gravity anomaly by genetic algorithm technique

Attempts to model potential fields expected to precede and accompany volcanic eruptions often involve a great deal of effort due to the complexity

of the considered problem. The inversion problem deals with the identification of the parameters of a likely volcanic source that leads observable changes in potential field data recorded in volcanic areas. Indeed, investigations on the analytical models describing the involved geophysical processes, have revealed that the models are highly non-linear and, usually, characterized by several parameters. When non-linear models are involved, the inverse problem becomes difficult to solve through local optimization methods. Hence, elaborated inversion algorithms have to be implemented to efficiently identify the source parameters. We have investigated the use of Genetic Algorithms⁶ (GAs) which perform a broad search over the parameter space using a random process with the aim of minimizing an objective function that quantifies the misfit between model values and observations. The GAs inversion strategy was applied on a gravity anomaly that grew up progressively in 5 months before the 2001 flank eruption of Mt. Etna along a East-West profile of stations on the southern slope of the volcano.⁷ Between January and July 2001, the amplitude of the gravity change reached $80 \mu\text{Gal}$, while the wavelength of the anomaly was of the order of 15 km (Fig. 4).

Elevation changes observed through GPS measurements during a period spanning the 5-months gravity decrease, remained within 4-6 cm all over the volcano and within 2-4 cm in the zone covered by the microgravity profile. Since February 2001, an increase in the seismicity was observed,⁸ with many earthquake locations clustered within a volume at a depth of about 4 km bsl and focal mechanisms pointing towards a prevailing tensile component. Therefore, we review both gravity and elevation changes by the Okubo model⁹ which mathematically describes the effect of uniformly distributed tensile cracks on gravity and ground deformation field in an elastic homogeneous half-space medium.¹⁰ The gravity solution consists of four contributions: (i) the free-air effect proportional to the uplift, (ii) the Bouguer change caused by the upheaved portion of the ground, (iii) the gravitational attraction of the crack-filling matter and (iv) the gravity field due to the redistribution of mass associated with the elastic displacements. This model implies inversion for nine parameters, $m = (A, X, Y, Z_1, Z_2, L, W, U, \delta\rho)$, whose description is reported in Table 1. To make the GA converge towards a solution which (i) best fits the observed data and (ii) has a good chance to be realistic from the volcanological point of view, we suitably restrict the parameter space to be investigated. The ranges of variability for the model parameters to be found are set on the grounds of the available geophysical and geological evidence. For the inversion procedure adopted in

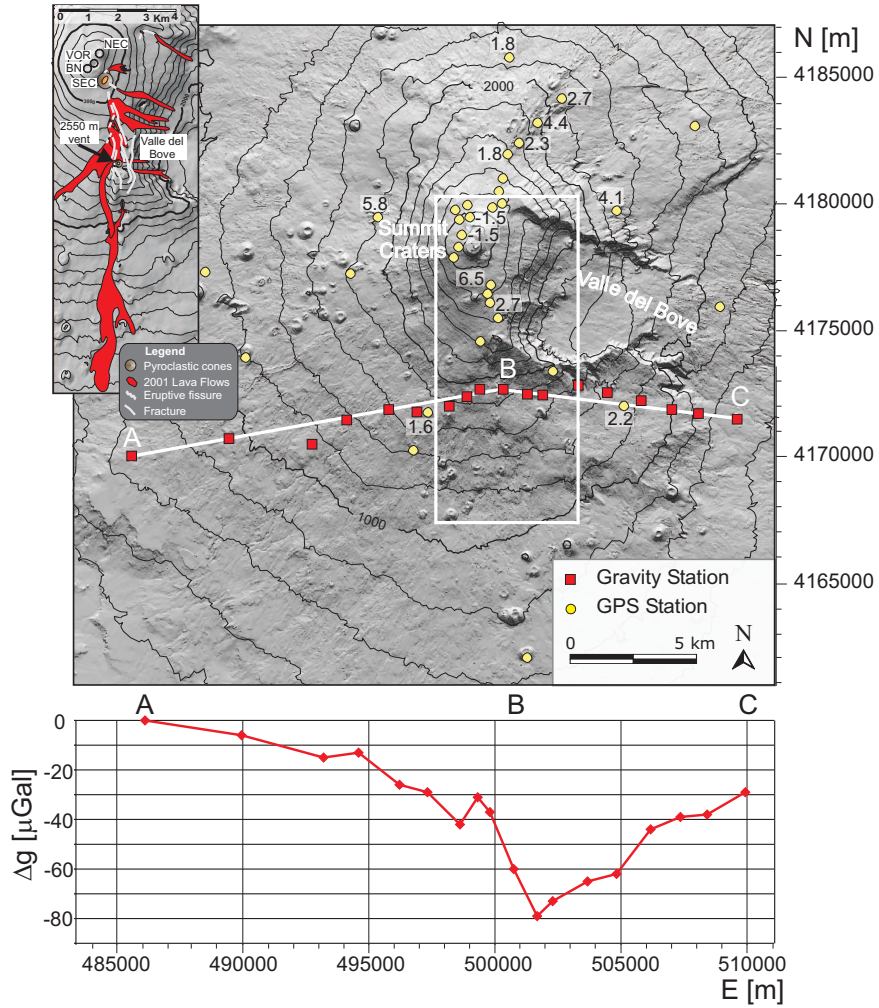


Fig. 4. Sketch map of Mt. Etna. Top: the gravity stations of the microgravity network along the East-West Profile (ABC) and the GPS stations measured in July 2000 and June 2001. The elevation changes higher than 1.5 cm, observed during the same interval, are also reported. The inset on the left shows the 2001 lava flow. Bottom: gravity change observed between January and July 2001 along the East-West Profile.

the present study, we have set the objective function equal to the χ^2 value that accounts for the measurements error defined by the standard deviation σ , as:

$$\chi^2 = \sum_k \frac{(M_k - C_k)^2}{\sigma_k^2} \quad (5)$$

where M_k are the measured data, C_k are the computed gravity variations and k is the number of available measurements. The parameters of the best model found through the GA are reported in Table 1, together with the edge values of each search range.

Table 1. The best model parameters found by the GA.

Parameter	Minimum	Maximum	Best value
Z ₁ - Depth of the top (m b.s.l.)	0	2500	409
L - Length (m)	1000	5000	5000
H - Height (m)	3000	7000	7000
W - Thickness (m)	500	2000	500
A - Azimuth (from the North)	-45	0	-30
X - Northing Coordinate(m)	4170000	4180000	4173940
Y - Easting Coordinate(m)	4950000	5050000	503499
$\delta\rho$ - Density contrast (kg/m ³)	-2400	-2700	-2500
U - Extension (m)	0	2	2

The fit between observed and calculated gravity changes is very good (Fig. 5), with a residual of 7.43 μGal , well within the error on temporal gravity differences along the East-West profile (10 μGal at the 95% confidence interval). Some of the best values found by the GA correspond to one of the edge value of the corresponding search range. This is in principle not ideal since it states for the GA to have been unsuitably confined during its search procedure. A sensitivity analysis of the parameters whose best value coincides with an edge of the chosen range is accomplished. Sensitivity tests are computed for the L-H and W-U couples of parameters, while the other remaining parameters are held fixed at their best values. The tests highlighted that while U is a highly sensitive parameter, W appears not to be so much sensitive. This observation reflects the assumptions behind the model: U defines the volume increase (volume of new voids, if the density of the filling material is set to zero) predicted by the model, while W only changes the volume within which the new fractures are uniformly distributed. In principle, changes of W do not influence the net effect of the model-body, if W remains much smaller than the depth of the mass center of the body itself. As for the L and H, they are sensitive parameters and the obtained best values appears to be a good compromise between the needs of (a) not

rising the value of these parameters towards an implausible extent and (b) assessing a satisfactory fit. In conclusion, the sensitivity tests confirm that the GA accomplished its task satisfactorily. Results show that, although it is possible to explain the observed gravity changes by means of the proposed analytical formulation, calculated elevation changes are significantly higher than observed. This finding could imply that another mechanism, allowing a significant density decrease without significant deformation, coupled the tensile mechanism due to the formation of new cracks, increasing the negative gravity effect while leaving the displacements at the surface unchanged. The only mechanism allowing a density decrease at depth without surface displacements is the loss of mass from a magma reservoir. To keep the maximum elevation change within 2-4 cm, a value of extension U less than 1 m should be assumed.

Using this value as an upper bound for the extension of the fracture zone, only about 50% of the observed gravity decrease can be explained using the Okubo model. Under the assumption that the new-forming tensile cracks and the loss of mass come from the same inferred source, it results that an about 10^{11} kg mass should be lost to contribute the missing 50% of the observed gravity decrease. The estimated mass corresponds to a minimum magma volume of $35 \cdot 10^6$ m³. It is worth to note that, during late 2000 and the first months of 2001, an almost continuous activity, with lava emission and Strombolian explosions from the summit Southeast Crater (SE), was observed.¹¹ The volume of the products emitted between January 2001 and the start of the main flank eruption is estimated to range between 13 and $20 \cdot 10^6$ m³. On the basis of our calculation, the volume emitted from the SE crater is of the same order of magnitude as the volume lost from the estimated gravity source. The hypothesis that the volume emitted from the summit SE crater, during the January-June 2001 period, was supplied by the same source in which tensile cracks formed needs to be further investigated to understand (i) which phenomenon could have triggered the mass transfer from the deep source volume to the surface and (ii) how this phenomenon relates to the formation of tensile fractures.

4. Conclusion

We illustrate two procedures dealing with linear and non-linear inversion of potential field data. Although the inversion problem suffers from the ambiguity and instability of its solutions, numerical methods allow for narrowing the set of all possible solutions and providing a unique and stable solution. As for large-scale linear inverse problem, a 3D inversion of magnetic field

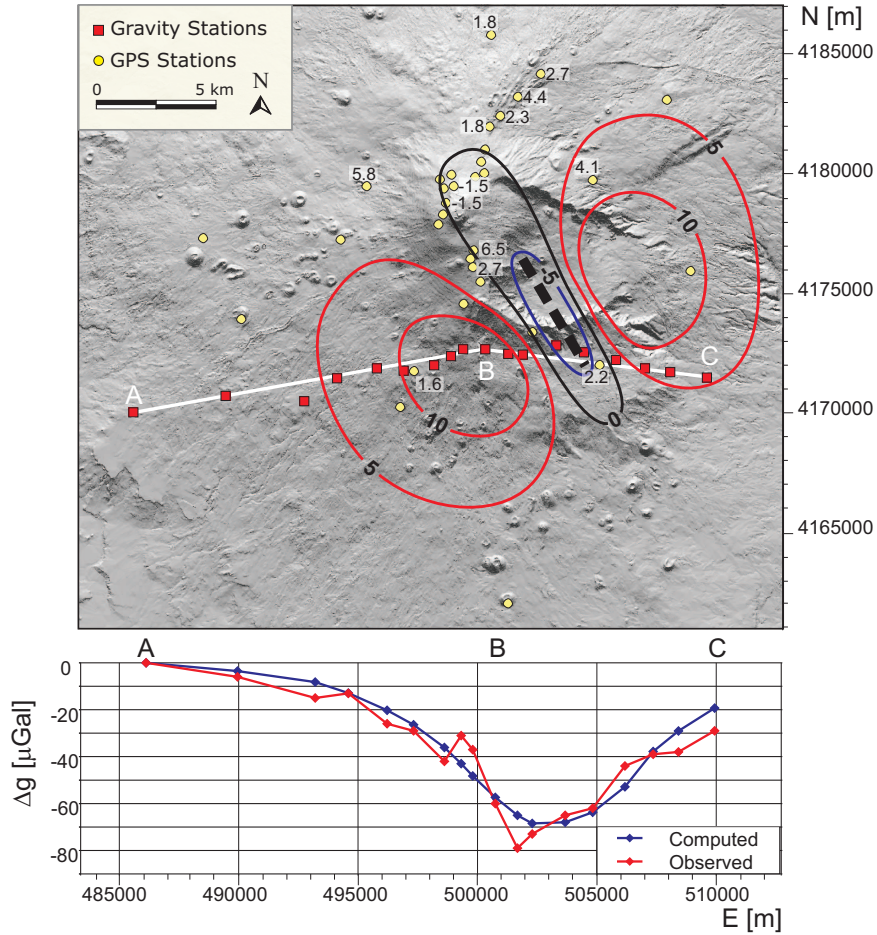


Fig. 5. Results based on the best model. Top: contour map (at 5 cm intervals) of computed elevation changes; surface projection of the source (dashed line); observed (July 2000 - June 2001) elevation changes higher than 1.5 cm. Bottom: observed (January - July 2001) and computed gravity anomalies.

data was performed by means of QP algorithm to produce a magnetization model that provides useful information of the subsurface geological structure of Ustica volcanic complex. As for non-linear potential field inversion, a GA technique was proposed to infer the parameters of a volcanic source that justifies the growth of a negative gravity anomaly preceding the 2001 Etna eruption. Our findings demonstrate that the identification and interpretation of potential field data can be a useful instrument both for de-

tecting subsurface geological structure model and improving the monitoring of active volcanoes.

References

1. R. J. Blakely, *Potential Theory in Gravity and Magnetic Applications* (Cambridge University Press, New York, 1995).
2. M. Fedi and A. Rapolla, *Geophysics* **64**, 452 (1999).
3. D. B. Rao and N. R. Babu, *Geophysics* **56**, 1729 (1991).
4. P. Gill, W. Murray, D. Ponceleon and M. Saunders, *Solving reduced KKT systems in barrier methods for linear and quadratic programming*, Technical Report SOL 917, Stanford University (Stanford, CA, 1991).
5. R. Napoli, G. Currenti and C. Del Negro, *Bull. Volc.* **in print** (2006).
6. G. Currenti, C. Del Negro and G. Nunnari, *Geophys. J. Int.* **162**, 1 (2005).
7. G. Carbone, D. Budetta and F. Greco, *J. Geoph. Res.* **108**, 2556 (2003).
8. A. Bonaccorso, S. D'Amico, M. Mattia and D. Patane, *Pure. Appl. Geophys.* **161**, 1469 (2004).
9. S. Okubo and H. Watanabe, *Geophys. Res. Lett.* **16**, 445 (1989).
10. D. Carbone, G. Currenti and C. Del Negro, *Bull. Volc.* **in print** (2006).
11. N. C. Lautze, A. J. L. Harris, J. E. Bailey, M. Ripepe, S. Calvari, J. Dehn, S. K. Rowland and K. Evans-Jones, *J. Volcan. Geotherm. Res.* **137**, 231 (2004).